

PAPER • OPEN ACCESS

## Physical and mechanical properties of burnt-out coal mine waste heaps

To cite this article: V K Kostenko *et al* 2024 *IOP Conf. Ser.: Earth Environ. Sci.* **1415** 012009

View the [article online](#) for updates and enhancements.

# Physical and mechanical properties of burnt-out coal mine waste heaps

V K Kostenko<sup>1</sup>, O P Bohomaz<sup>1</sup>, M I Tavrel<sup>1</sup>, I O Hlushko<sup>1</sup> and T V Kostenko<sup>2</sup>

<sup>1</sup> Donetsk National Technical University, Department of Environmental Protection, 56 Potebni Str., Lutsk, 43003, Ukraine

<sup>2</sup> Cherkasy Institute of Fire Safety named after Chernobyl Heroes of National University of Civil Defence of Ukraine, Department of Construction Objects Safety and Labor Protection, 8 Onoprienka Str., Cherkasy, 18034, Ukraine

E-mail: viktor.kostenko@donntu.edu.ua, olha.bohomaz@donntu.edu.ua, maryna.tavrel@donntu.edu.ua, inna.hlushko@donntu.edu.ua, tatiana.kostenko@gmail.com

**Abstract.** Currently, the issue of finding new ways to process, utilize and reuse burnt-out waste heaps in order to reduce their technogenic impact on the environment becomes relevant. The presence of a porous structure in combination with undissolved properties opens up the possibility of using the burnt-out mine rock to make composite fertilizers to improve the quality of agricultural and technogenically degraded soils. The widespread use of burnt-out mine rock for the manufacture of composite soils requires the study of their physical and chemical properties and deformation characteristics. In laboratory conditions, the physical and mechanical properties of samples of burnt-out rock masses ranging in size from 1.25 to 10 mm with and without the addition of powdered soil under a load of up to 110 kN were studied. For the first time, a certain increase in load resistance was found when soil powder was added in the initial period of compression of the tested material. It was determined that the destruction of particles of burnt-out material occurs in two waves. These results indicate the presence of two strength limits in the burnt-out medium composed of two initial petrotypes.

## 1. Introduction

The coal industry of Ukraine is one of the most important branches of the mining industry, since it is the main supplier of raw materials for domestic power and metallurgical enterprises, as well as an exporter of extracted products to world markets [1]. Despite the trend towards popularization of alternative energy sources, it is expected that the intensity of coal mining will increase annually due to the demand for energy raw materials in the world [2], which is associated with the energy crisis, rapid industrialization, and population growth [3].

Underground coal mining causes various environmental problems that cause significant damage to the environment and natural biocenoses. These problems include exogenous and endogenous fires [4], methane emissions [5], water pollution by mine wastewater, surface subsidence, destruction of biodiversity [6], and soil degradation [7]. A special part is played by the problem of solid mining waste management, which often contains substances that are harmful and hazardous for the environment [8], and their deposition contributes to dust and toxic gas emissions, as well as toxic solution washing-off.



The practice of coal mining enterprises has shown that one ton of coal produces about 0.4-0.5 tons of waste rock. This figure is an average and may vary depending on the quality and strength of the coal seam. Thus, for coal basins in Ukraine, this figure is in the range of 0.12-0.39 tons, and 0.4-0.5 tons in Poland [9].

Modern mining technologies used in different coal-producing countries are mainly aimed at the fullest possible extraction of coal from the longwall [10] and accumulation of waste rock in the mine working space without recovering it to the surface [11]. This method minimizes the amount of solid waste generated during coal mining and reduces the technogenic impact on the environment. However, just like 20-40 years ago, most coal mines in Ukraine continue to operate according to the old scheme: the bulk of the waste rock is not utilized but is placed near coal mines, forming waste heaps of various configurations. This has led to the accumulation of more than 25 billion tons of solid mining waste in the country's coal mining regions [12], which is stored in more than 1,000 waste heaps [13].

Waste heaps cause significant environmental damage. Being under the constant influence of climatic factors, their surface is subject to wind and water erosion, as a result of which dust, as well as oxidized compounds of sulphur, iron, carbon and other harmful elements, enter water bodies [14] and adjacent agricultural soils, thereby contaminating them [15].

However, the greatest danger of waste heaps is their fire and explosion hazard. This is especially true for old heaps. This is due to the fact that chemical and biological processes in the waste mass, involving pyrite and coal, have been occurring for many years with the release of elevated temperatures and are often accompanied by smouldering, burning [16], and sometimes explosions [17]. Such fires are a source of dust and gaseous substances emitted into the atmosphere, and the high temperatures [18] accompanying the fires pose a threat to the population within the radius of the waste heaps [19]. Therefore, the issue of finding new ways to process, utilize and reuse burnt-out waste heaps in order to reduce their technogenic impact on the environment becomes relevant.

## 2. Literature review

Waste heaps in the coal basins of Ukraine mostly consist of a coarse mixture of mudstones, siltstones, sandstones, pyritized and other types of rocks with a number of components, such as aluminium, zinc, sulphur, titanium, molybdenum, which is why they can be considered as valuable secondary deposits. The direction of possible reuse of waste heaps is determined by the physical and chemical characteristics of the waste mass. However, during prolonged burning, under the influence of high temperatures (1000...1200 °C), changes occur in the structural characteristics of the original rock, which leads to the formation of new material from the waste mass of varying degrees of burning-out: from sintered to slightly burnt, with different strength, water permeability and porosity. These indicators should be taken into account when determining promising areas for further use of burnt-out mine rock.

Burnt-out waste from coal enterprises has great potential for use in the construction sector [20]. Thus, studies have shown the prospects of using burnt-out mass for the manufacture of porcelain stoneware [21], cement mixtures, modified building insulation materials, and materials for backfilling mine workings [22].

It is recommended to use burnt-out mine rock in a concentration of 50% for the manufacture of modified foundations. Due to the use of modified material from burnt-out solid waste, which has stable characteristics, the bearing capacity and strength of foundations constructed on loess soils increases [23]. For buildings constructed in areas that are prone to surface subsidence, such as over mine shafts, it is recommended to use a three-layer slab foundation, in which one layer is made using burnt-out rock. In this case, the use of burnt-out waste rock will not only increase the reliability of buildings but also improve the environmental situation in the coal mining region.

Given the shortage of local natural stone raw materials, the use of burnt-out waste heaps in coal mining regions for the construction of structural layers in the construction of pavement is of particular relevance [24], or for the creation of subgrade in the levelling of sites [25]. This minimizes the costs associated with the extraction and transportation of stone raw materials.

The presence of a porous structure in combination with undissolved properties opens up the possibility of using both burnt-out and common mine rock to make composite fertilizers to improve the quality of agricultural and technogenically degraded soils. To do this, the rock is mixed with an organic component, which can be municipal sewage sludge or water body silt. Studies have shown that the addition of coal industry waste and its mixtures with municipal sewage sludge and rock wool waste improves soil pH and its occlusion properties [26]. Laboratory studies have confirmed that the creation of a nutrient mixture based on 25% burnt-out mine rock, 25% river silt, and 50% degraded loamy black soil treated with red California worms allows for 100% germination of tomatoes, unlike other substrates that did not contain burnt-out rock [27].

However, the widespread use of burnt-out mine rock for the manufacture of composite soils requires the study of their physical and chemical properties and deformation characteristics.

The purpose of this paper is to evaluate the effect of particle size distribution on the physical and mechanical properties of burnt-out waste rock.

### 3. Research methods

The study of the physical and mechanical properties of experimental samples of burnt-out rock mass was based on DSTU BV.2.1-4-96 “Soils. Methods of laboratory determination of strength and deformation characteristics” [28].

The process of deformation of the mixture of burnt-out waste mass and soil was studied. Samples for the study of rock properties were taken from the non-operational heap of mine No. 5/6 of the Myrnohraduhillya Production Association (Myrnohrad). The rock was sampled at five points from a depth of up to 10 cm using the “envelope” method. The sampling site had no signs of intense oxidation, burnt zones, etc. The initial waste mass was represented by interspersed layers of siltstones and mudstones (sand shales) with sandstones. In the burnt-out state, their residues were: dark – siltstones, light grey – mudstones and sandstones. The gradual burning-out of rocks occurred slowly over several decades under the influence of atmospheric processes: oxygen, moisture, wind, bacteria, temperature changes, etc. The largest of the selected pieces were crushed mechanically. After crushing the rock, the resulting particles were separated using laboratory sieves into fractions, *mm*: 10...5; 5...3; 3...1.25. Preliminary laboratory studies have shown that the burnt-out mine rock of larger fractions have characteristics which not suitable manufacture of composite soils. Therefore, physical and chemical properties and deformation characteristics was carried out only for fractions 10...5; 5...3; 3...1.25.

Each rock fraction was microscopically examined using a monocular microscope XSP – 128 and a camera Levenhuk M1000 PLUS. The magnification of the images was the same. To compare the geometric dimensions of the inclusions and the parameters of irregularities and pores, a 0.02 *mm* Momoi Hameleon Extreme fishing line was included in the image composition as a geometric reference.

For both petrotypes, namely dark and light, the particle shape, the nature of its edges, the presence of visual porosity, cracks and faults were assessed for each fraction.

To determine the deformation characteristics of the rock in each fraction, 4 samples were prepared: a reference, without additives, and three samples each with the addition of loamy soil typical for the area with mass concentrations of 10, 20, and 30 percent. The soil additives in powder form were thoroughly mixed with the dried rock. The weight  $m$  (*g*) of the samples and their bulk density  $\rho_{pb}$  ( $g/cm^3$ ) were determined by the weight method (table 1). The table

shows that the addition of soil powder led to an increase in the density of the mixture compared to the ‘pure’ (0 percent additive) rock by 0.03...0.15 ( $g/cm^3$ ). However, the difference in this indicator, when adding 10...30 percent (wt.) of soil, was within the measurement error.

**Table 1.** Data of laboratory studies for determining the bulk density and weight of the studied samples of burnt-out mine rock.

Percentage of soil in the mixture, %	Fraction size, mm					
	5...10		3...5		1.25...3	
	$m, g$	$\rho_{pb}, g/cm^3$	$m, g$	$\rho_{pb}, g/cm^3$	$m, g$	$\rho_{pb}, g/cm^3$
0	290	1.08	281	1.04	301	1.12
10	300	1.11	320	1.19	326	1.21
20	300	1.11	320	1.19	326	1.21
30	300	1.11	320	1.19	320	1.19

The prepared samples were placed in a steel cylinder (figure 1) with a diameter of  $d=7.5\text{ cm}$  and a height of  $h=6.1\text{ cm}$ . The steel cylinder with samples of burnt-out mine rock was covered with a massive metal plunger and placed between parallel press plates and subjected to loading.

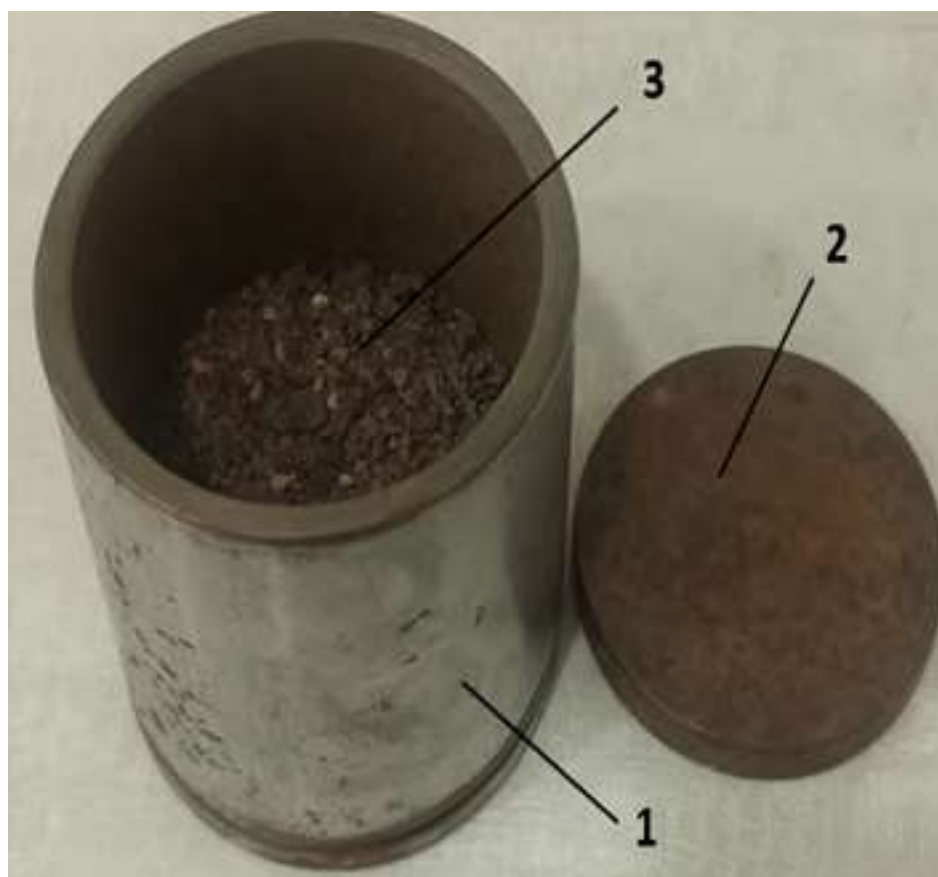


**Figure 1.** Device for experimental determination of deformation characteristics of burnt-out mine rock: 1 – steel cylinder, 2 – plunger, 3 – experiment sample.

The deformation characteristics were determined using a press P-50 (figure 2, a). The loading speed was automatically adjusted to 0.21  $m/s$ , and the loading force of the samples was increased

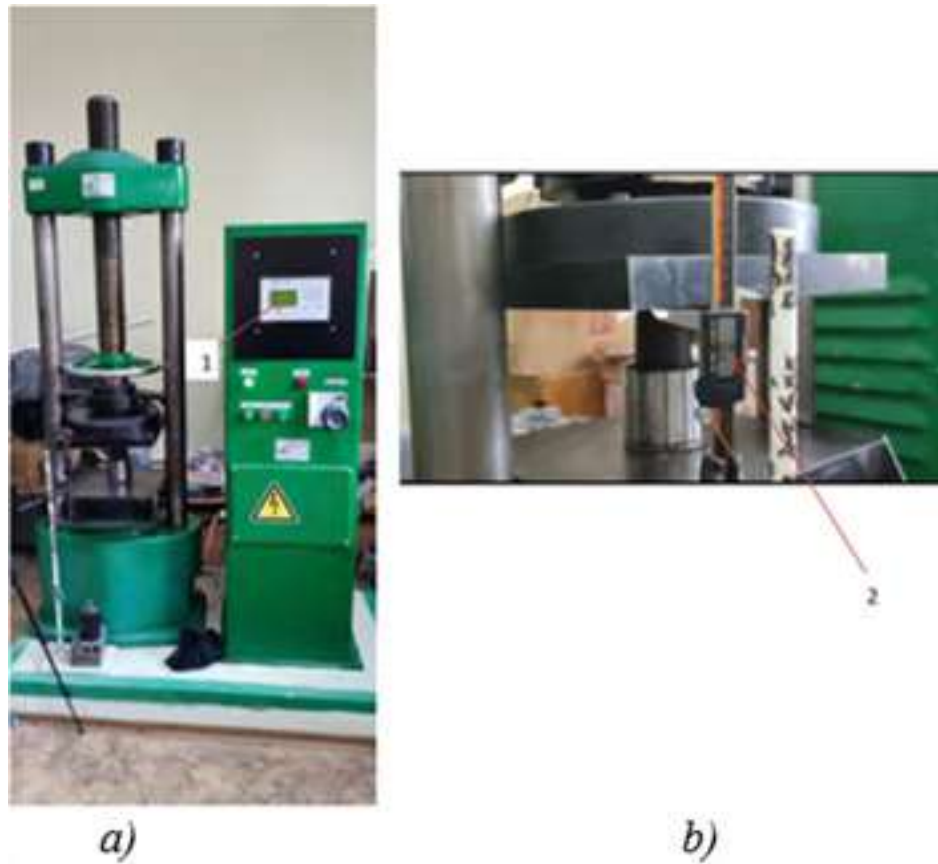


**Figure 2.** Laboratory setup for measuring the deformation properties of soils: *a)* – general view of the P-50 hydraulic press, 1 – indication of the compression force,  $F$ ,  $N$ ; *b)* – strain measurement unit, 2 – indication of plate convergence  $\Delta h$ ,  $m$ .

from 0 to 110  $kN$ . At the same time, the convergence of the press plates was recorded (figure 2, *b)*), which corresponded to the deformation of the sample. The experiment was timed using a laboratory stopwatch.

The task of the observations was to record the dynamics of changes in the height of the sample  $\Delta h$ ,  $m$ , which corresponded to the action of a certain value of the compressive force  $F$ ,  $kN$ .

The test results were processed using the following formulas. Relative vertical deformation of the sample  $\varepsilon$ :

$$\varepsilon = \frac{\Delta h}{h} \tag{1}$$

where  $\Delta h$  is the value of the vertical absolute deformation of the sample under load,  $m$ ;  $h$  is the initial height of the sample,  $m$ .

Energy  $E$ ,  $J$ , which was spent on compressing the sample to a value of  $\Delta h$ :

$$E = F \cdot \Delta h, J, \tag{2}$$

where  $F$  is the sample compression force,  $N$ .

Pressure in the rock sample  $P$ ,  $Pa$ :

$$P = \frac{F}{S}, Pa, \tag{3}$$

where  $S$  is the cross-sectional area of the cylinder,  $m^2$ .

Power  $W$ ,  $W$ , of compression of the sample:

$$W = \frac{E}{t}, W, \quad (4)$$

where  $t$  is the duration of the loading process,  $s$ .

#### 4. Research results

The results of microscopic examination of particles of different fractions are shown in figure 3 and table 2.

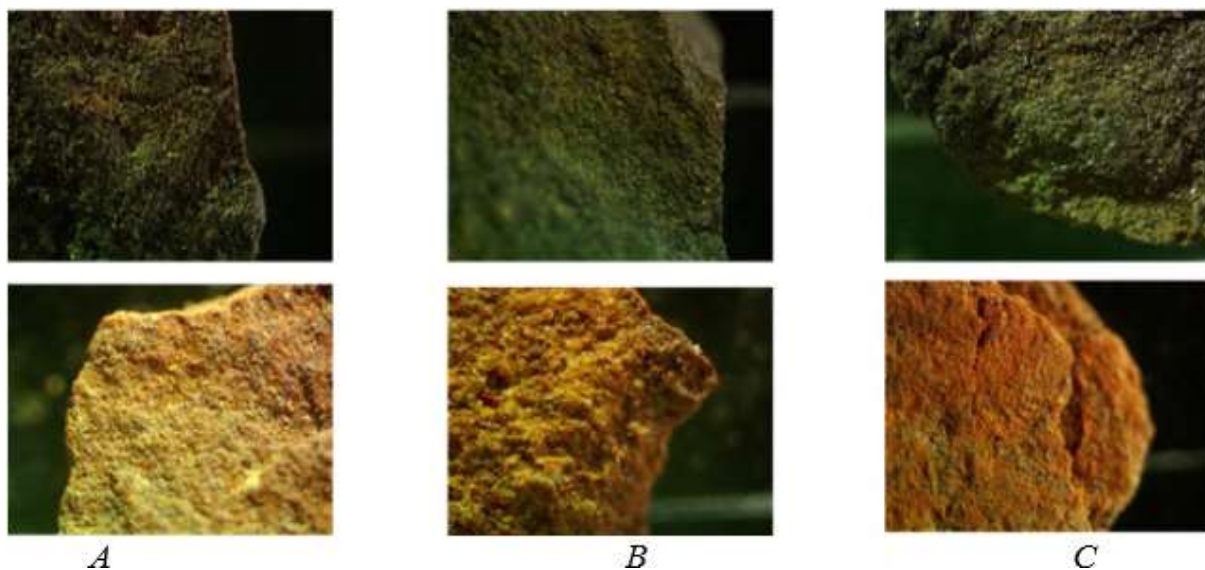


**Figure 3.** Microscopic images of rock samples, dark: mudstones, light: siltstones and sandstones:  $A$ ,  $B$ ,  $C$  – respectively, fractions ( $mm$ ), 10...5, 5...3, 3...1.25.

The particles of the 10...5  $mm$  fraction (figure 3,  $A$ ) of the rock have a pronounced flat shape with a diverse geometric structure. The edges of the particles are rounded with uneven protrusions. The surface is porous with a small number of depressions, there is a significant number of inclusions of yellow colour, a smaller amount of orange and black; no cracks are observed. The relatively uniform nature of the surfaces indicates a low probability of air bubbles accumulation on them, and air retention is possible mainly in the space between rock particles.

The rock particles of the 5...3  $mm$  fraction (figure 3,  $B$ ) have both flat and three-dimensional shapes, resembling pyramids and parallelepipeds. The edges of the particles have the shape of sharp angles, and the protrusions of inclusions are pronounced. The porosity of the rock surface is increased, there is a large number of mineral inclusions of yellow, orange and white colour; no cracks are observed. The light-coloured particles are characterized by a pore-like texture, which may contribute to the retention of air bubbles covered with suspension.

The particles of the 3...1.5  $mm$  fraction (figure 3,  $C$ ) have three-dimensional shapes, the vast majority resembling grains and pyramids. The edges of the particles are rounded with faults, and inclusion protrusions are pronounced. The porosity of the rock surface is increased. A large number of inclusions: yellow, orange, white, black and transparent. Cracks and faults are observed on both dark and light-coloured particles, which can serve as air collectors.

**Table 2.** Characteristics of the fractions of the studied samples of burnt-out mudstones and siltstones.

Particle characteristics	Fraction, <i>mm</i>					
	10...5		5...3		3...1.5	
Initial rock	mudstone	siltstone	mudstone	siltstone	mudstone	siltstone
Shape	flat		flat and three-dimensional		three-dimensional	
Shape edge	rounded	sharp corners	pronounced sharp corners		rounded	
Porosity	porous	porous	increased porosity		increased porosity	
Cracks	–	–	–	–	+	+
Faults	+	–	–	+	+	+
Inclusions of a certain colour*, %						
Yellow	22	38	18	42	28	34
Orange	2	5	–	16	5	8
White	–	–	6	8	4	9
Black	–	11	–	–	–	8
Transparent	11	–	10	–	9	18

\* Inclusions are calculated in % of the total area of the studied rock surface of a certain fraction.

From the results presented in table 2, it follows that particles with a size of 10 to 3 *mm* are characterized by a flat (scaly) shape, they are porous, there are no cracks, and there are stepwise faults.

Smaller particles are characterized by a rounded shape, greater porosity, and a higher frequency of cracks and faults. Unlike others, the 5...3 *mm* fraction is characterized by sharp edges, which may affect the nature of the deformation process. In the larger fraction, the presence of sharp protrusions is less pronounced.

According to the results of force tests, it was found that there is a parabolic relationship between the energy expended on the compression of the rock sample and its deformation (figure 4). It is valid for all types of the tested samples. At the beginning of loading, deformation occurs at a high rate. Thus, 50 *J* was sufficient to achieve a vertical deformation of  $\Delta h = (0.014...0.018)$  *m*. However, at a level of more than 50 *J*, a sharp increase in the energy required to reduce the height of the sample is observed. At a load in the range from 50 to 250 *J*, the level of additional deformation was only about  $\Delta h = 0.01$  *m*.

The addition of soil to the fraction of 1.25...3 *mm* in the amount of 10% did not significantly affect the deformation pattern of the sample (figure 4, *A*), which did not differ from the deformation of pure rock. An increase in the soil additive to 20...30% led to an increase in the value of  $\Delta h$  by about 0.005 *m* at the initial stage, with a load of up to 50 *J*. With further loading, the deformation dynamics was the same for all samples.

All samples of the 3...5 *mm* fraction were compressed in a single movement (figure 4, *B*) as a whole. A similar pattern is also characteristic of samples of 0, 10, 20% of the 5...10 *mm* fraction (figure 4, *C*). At the initial period of loading (up to 50 *J*), a close to  $\Delta h = 0.002$  *m* increase in deformation is inherent in the sample with the addition of 30% soil.

For almost all tested samples, the final deformation was about  $\Delta h = 0.02...0.025$  *m* at a loading energy of 250 *J*. The exceptions were samples of 0 and 10% of the 1.25...3 *mm* fraction, where this indicator was  $\Delta h = 0.016...0.018$  *m* (figure 4, *A*).

It should be noted that the ‘power-deformation’ diagrams reflect the reaction of the samples to the force impact of the loading setup. Of interest are the dependencies between the load and the power spent at this pressure in the test material. Such dependencies show the dynamics of deformation of the dispersed medium under uniaxial vertical loading with a horizontal



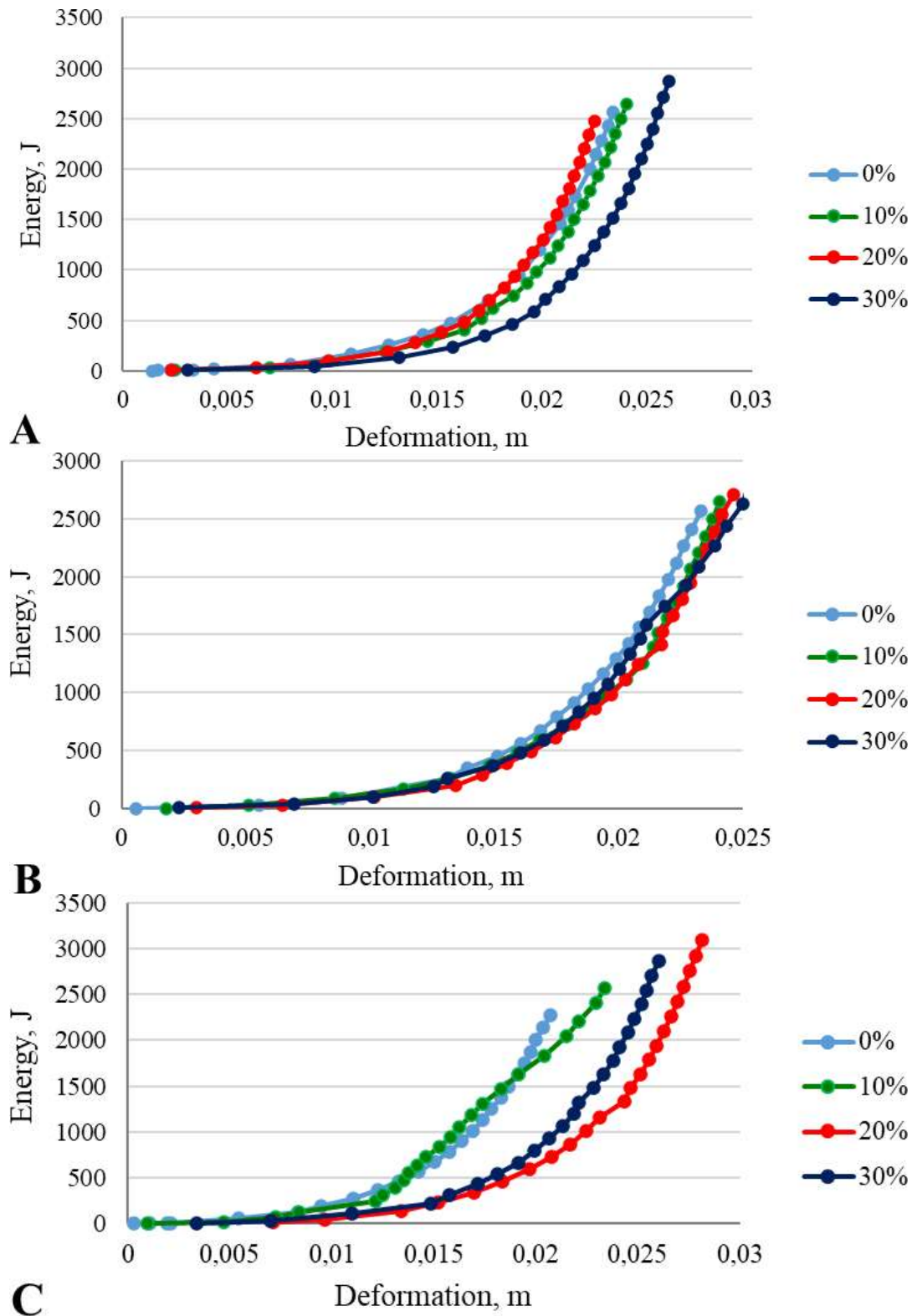


**Figure 4.** Energy ( $J$ ) spent on deformation ( $\Delta h, m$ ) of the samples:  $A, B, C$  – respectively, fractions ( $mm$ ), 1.25-3; 3-5; 5-10.

displacement limit. The results of the study in the form of 'power-pressure' diagrams are shown in figure 5. The results obtained are visually strikingly different from those shown above. There are no smooth lines, and their synchronous location. The graphs illustrating the dependence of the power required to compress the sample are characterized by a broken form, and in many cases, there are extremes. It is known that line bends, and especially the presence of extreme points, indicate a qualitative change in the nature of the process under study.

It can be assumed that the change in the deformation mode of the sample is caused by the accumulation of potential energy in the rock particles and the mutual sliding of the particles of the discrete medium, as well as the transition of the potential energy accumulated in the particles to kinetic energy by breaking the particles and subsequent movement. Particle breaking can occur by separating sharp edges, separating rounded particles, etc. Due to the chaotic arrangement of particles in the steel cylinder (figure 1), individual elements of the process of rock particle movement and breaking are not clearly reflected in the graphs, but when a common phenomenon characteristic of the sample scale occurs, it manifests itself in the form of bends or extremes.

The analysis of the results of loading rock samples without the addition of soil powder is indicative. The power increase in the largest (5...10 mm) fraction (figure 5, A, item 1) was observed linearly with an approximately uniform rate up to the level of 7 W and a pressure of about 3800 kPa, after which the power increase rate decreased until the end of the experiment ( $W=9$  W,  $P=5800$  kPa). It can be assumed that at the initial stage, the energy of rock particles was accumulated, accompanied by simultaneous particle breaking and the appearance of small particles. Subsequently, after reaching a high pressure level comparable to the tensile strength of the material, the process of breaking with particle movement has intensified, but the required power increase has decreased.

It should be noted that the absence of powder provided a high level of contact stresses between the particles, which contributed to their intensive breaking. This is indirectly confirmed by the test graphs of samples of 5...10 mm fraction with the addition of powder; all lines (figure 5, A, items 2, 3, 4) are above the line of pure rock. In the samples with the addition of soil, due to the increase in the contact areas of energy accumulation, an intensive increase in power occurred at the initial stage without significant crushing and sliding of particles.

When loading the samples of clean rock of 3...5 mm fraction (figure 5, B, item 1), an intensive power increase occurred to a level of about 7 W and a pressure of up to 1800 kPa, after which there was a slight decrease to 6 W at 2000 kPa. It should be noted that the number and area of contacts between the particles in this fraction is much smaller than in the previous one, so the difference between the pure rock and the one with additives is not so significant. This indicates that up to a certain level of load, the particle crushing was of a small scale, and after reaching a certain limit, breaking and sliding occurred. The power level of such a limit was 6...8 W, i.e., close to that when loading a larger fraction at 1500...2000 kPa (figure 5, B, items 1, 3).

The deformation pattern of the sample of the 1.25...3 mm fraction was close to that of the coarse fraction, the graph curve (figure 5, C, item 1) is similar to (figure 5, A, item 1), only the bend point had the coordinates  $W=10$  W,  $P=4000$  kPa, which can be explained by a larger number of contacts between small particles and, therefore, a lower level of contact stresses at the same pressure level.

The presence of powder in the mixtures reduced the destructive role of contact stresses, which sometimes required higher power levels for loading at relatively low stresses (figure 5, A, item 3, figure 5, B, item 2, figure 5, C, item 4).

In the process of loading, more than half of the samples of the three fractions showed a rapid increase in pressure to a level of about  $P=1500$ ...1800 kPa and power to  $W=7$ ...11 W, followed by an increase in pressure to  $P=2000$ ...2200 kPa accompanied by a decrease in power level by 2...3 W, sometimes more. Subsequently, the increase in power and pressure occurred at

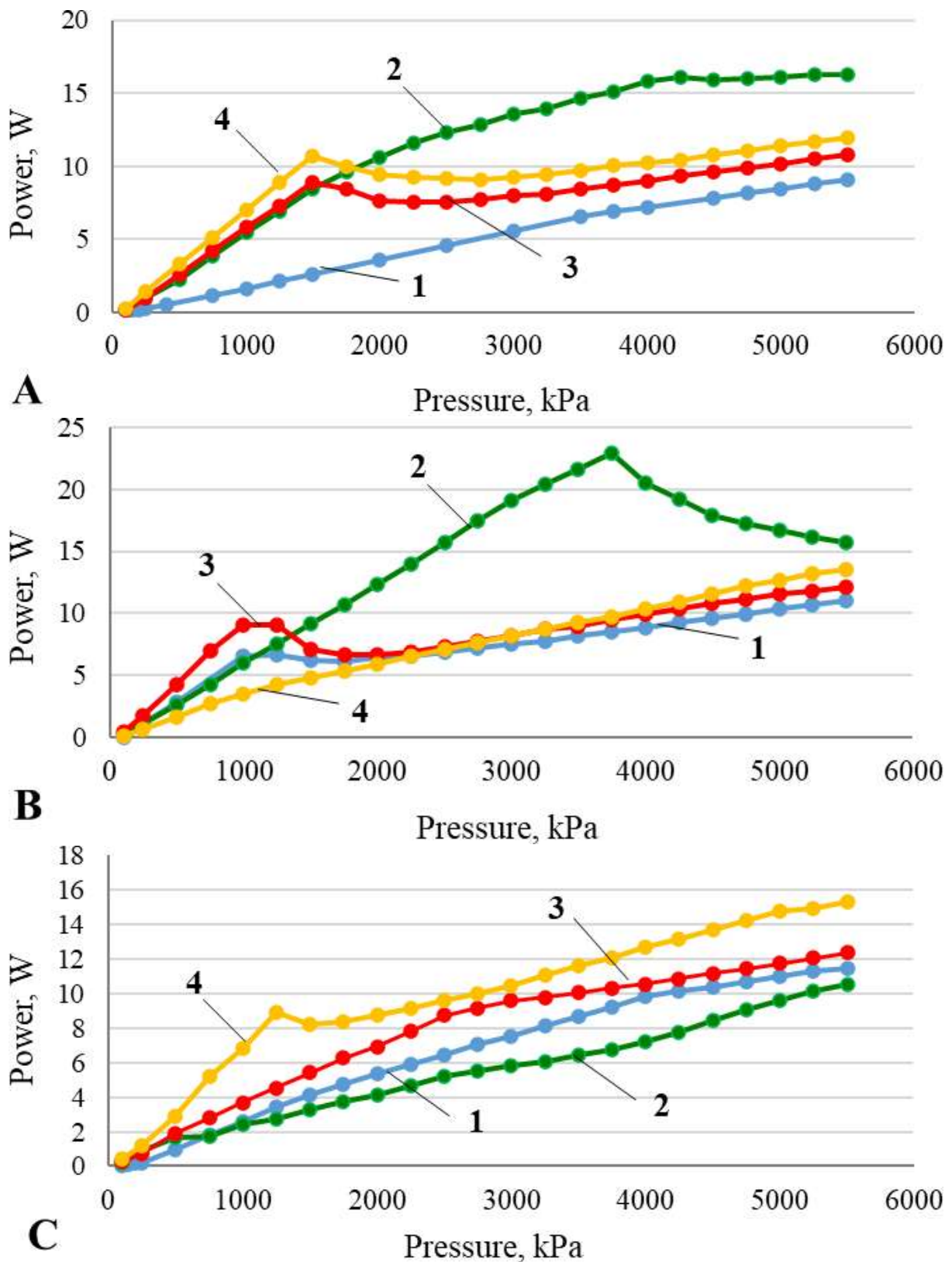


**Figure 5.** Power  $W$  (W) consumed to compress rocks to a pressure  $P$  (kPa): rock without additives; 2,3,4 – respectively, 10, 20, 30% of soil powder added: A, B, C – respectively, fractions (mm), 5-10; 3-5; 1.25-3.

a constant rate for all samples.

The reference rock samples of each fraction, after loading up to 110  $kN$ , were sieved and the percentage of rock that was crushed was determined (table 3). These data showed that a significant portion of the energy used to compress the rocks was spent on crushing the rock particles, and the rest on compacting the sample. The largest percentage of crushing is inherent in the larger fraction. Particle breaking occurs at the points of contact with neighbouring particles, when the level of contact stress exceeds the tensile strength. Such conditions are more likely to occur when larger particles interact due to a smaller number of contacts and a corresponding increase in contact forces. Such processes can be manifested in the form of an abrupt change in the  $\Delta h$  indicator. Moreover, the deformation of small fractions should be almost twice as smooth as that of large ones.

**Table 3.** Percentage of rock crushed after loading of the reference samples.

Fraction size, $mm$	Fraction weight, $g$		Proportion of crushed rocks, %
	before	after	
5-10	290	96.76	66.63
3-5	281	174.04	38.06
1.25-3	301	209.31	30.46

## 5. Discussion of the results

The study of the deformation properties of mixtures of rocks and powdered additives is necessary, e.g., for the construction of road bases using burnt-out rocks. The addition of a sufficient amount of powders that swell under the influence of water, such as montmorillonite, to gravel or crushed stone allows for creating a waterproofing ‘jacket’ that prevents water from penetrating the road body and deforming it during freezing and thawing. The availability of deformation data sheets for the mixture allows for establishing a consensus between the bearing capacity of the mixture and its waterproofing properties.

The results obtained revealed a certain increase in load resistance when soil powder was added during the initial compression period (figure 5). Almost all the lines of the graphs characterizing the power required for compression located above the line are characteristic of pure (0% soil additive) rock. This can be explained by the contact stress levelling effect due to the filling of voids with powder and, therefore, an increase in the interaction areas of rock particles. The destruction of rock particles was observed, in most cases, at a pressure of 1500...1800  $kPa$ , which is typical for burnt-out mudstones. After crushing such particles, their mutual sliding occurred with a slight decrease in the power required for further deformation. The next wave of particle crushing was observed when the pressure increased to an index approximately equal to 3800...4000  $kPa$  (figure 5, *A*, items 1, 3; figure 5, *B*, item 2; figure 5, *C*, items 1 and 3), which is typical for siltstones and sandstones. Subsequently, the rate of pressure growth slowed down. After the active destruction of rock particles was completed, the material consolidated and deformation of the samples occurred at almost the same rate. These results indicate the presence of two strength limits in the burnt-out medium composed of two initial petrotypes.

The methodology of the experiment did not provide for the registration of the process of rock breaking, only its results were reported (table 3). In the future, it would be advisable to observe mechanical and acoustic phenomena in the samples in parallel with the compression of the samples to clarify the periods of intense rock destruction. An additional disadvantage of the conducted research should be considered the limited scope of the experiments both in terms of the number of samples and the number of experimental objects, only one waste heap

was considered. This can be explained by the difficulty of working under martial law, and the shortcomings will be eliminated in the future.

Microscopic studies have shown the presence of various types of mineral components that make up burnt-out rocks. The photographs (figure 3) clearly distinguish inclusions of yellow, orange, white, black, and transparent colours (table 2). No mineral analysis of these inclusions was performed. However, based on the literature data, it is possible to provide a rough estimate that red and orange inclusions are typical for iron oxides, yellow – for sulphur compounds, white and transparent are quartzite, black are carbon compounds. This approach is very approximate and should be further refined. However, different types of minerals have different attitudes towards water, namely, they can be hydrophilic or hydrophobic. This is an important characteristic of the material in its practical use, so was evaluated the occlusion capacity of the burnt-out waste rocks of mine No. 5/6 [29]. Laboratory studies have shown that burnt-out rocks are able to retain a certain amount of liquid on their surface, the so-called film water ( $W_f$ ), as well as capillary water, which is retained in pores and cracks ( $W_C$ ). The latter indicator was defined as an increase in the moisture capacity of the rock ( $W_{RC}=W_f+W_C$ ) after prolonged (up to 24 hours) saturation with water that penetrated into cracks and capillaries in the rock particles (table 4).

**Table 4.** Fractional indicators of the capacity of film occluded and capillary water in burnt-out rocks.

Fraction, <i>mm</i>	$W_{RC}, \%$	$W_f, \%$	$W_f/W_{RC}$ , particle
5-10	8.08	6.96	0.86
3-5	12.58	11.36	0.90
1.25-3	13.60	12.96	0.95

The total moisture capacity  $W_{RC}$  increased from 8.08 to 13.6% relative to the mass of dry rock with decreasing fraction size. The occluding surface of larger particles (5-10 *mm*) was the smallest with the same weight of the experimental samples, so the film water indicator was the lowest. Experimentally, it was found that for a geometrically smaller fraction (1.25-3 *mm*), which is three to four times smaller, the  $W_{RC}$  indicator was about 40% higher.

The data obtained are also needed in the future to reveal the mechanism of deformation of a mixture of rocks with wet bottom sediments [30]. The thing is that in addition to solid and liquid components that are almost incompressible, the mixture may contain air. It is an elastic substance and affects the results of the experiment. When wet materials placed in a test vessel are loaded, the gases are not completely displaced, but migrate to pores, cracks, etc. When testing dry samples, this phenomenon is not observed, instead, moisture isolates the gaps between the particles and seals air bubbles, which change their volume during loading and unloading, which affects the deformation of the material. The test methodology does not provide for control of the presence of air in the test medium.

To assess the impact on the deformation of a mixture of rock and wet sediments, it is necessary to consider the possibility of air in the pores, cracks, and gaps between the particles. Visual observations and research show that in the process of burning-out, the waste masses become close in properties to ceramics; their particles do not increase in volume when wet.

## 6. Conclusions

In laboratory conditions, the physical and mechanical properties of samples of burnt-out rock masses ranging in size from 1.25 to 10 *mm* with and without the addition of powdered soil under a load of up to 110 *kN* were studied. For the first time, a certain increase in load resistance was found when soil powder was added in the initial period of compression of the tested material.

It was determined that the destruction of particles of burnt-out material occurs in two waves. The first wave was observed at a pressure of 1500...1800 *kPa*, followed by material sliding with a slight decrease in the power required for further deformation. The second wave was observed at a pressure increase of approximately 3800...4000 *kPa*.

It was also determined that after the active destruction of rock particles was completed, the material consolidation and deformation of the samples occurred at almost the same rate. These results indicate the presence of two strength limits in the burnt-out medium composed of two initial petrotypes.

### ORCID iDs

V K Kostenko <https://orcid.org/0000-0001-8439-6564>

O P Bohomaz <https://orcid.org/0000-0002-8521-0394>

M I Tavrel <https://orcid.org/0000-0002-7666-4554>

I O Hlushko <https://orcid.org/0009-0002-5283-1861>

T V Kostenko <https://orcid.org/0000-0001-9426-8320>

### References

- [1] Markevych K, Maistro S, Koval V and Paliukh V 2022 Mining sustainability and circular economy in the context of economic security in Ukraine *Mining of Mineral Deposits* **16**(1) 101–113 DOI <https://doi.org/10.33271/mining16.01.101>
- [2] Žuk P and Žuk P 2022 National energy security or acceleration of transition? Energy policy after the war in Ukraine *Joule* **6**(4) 709–712 DOI <https://doi.org/10.1016/j.joule.2022.03.009>
- [3] OECD 2019 *Global Material Resources Outlook to 2060: Economic Drivers and Environmental Consequences* (Paris: OECD Publishing) DOI <https://doi.org/10.1787/9789264307452-en>
- [4] Kostenko V, Zavialova O, Novikova Y, Bohomaz O, Krupka Y and Kostenko T 2022 Substantiating the parameters of quickly erected explosion-proof stopping *Rudarsko-geološko-naftni zbornik* **37**(4) 143–153 DOI <https://doi.org/10.17794/rgn.2022.4.12>
- [5] Kostenko V, Bohomaz O, Kostenko T and Berezovskyi A 2023 Mechanism of coal aerosol explosion development in an experimental mine working *Rudarsko-geološko-naftni zbornik* **38**(2) 135–142 DOI <https://doi.org/10.17794/rgn.2023.2.10>
- [6] Abramowicz A, Rahmonov O and Chybiorz R 2021 Environmental Management and Landscape Transformation on Self-Heating Coal-Waste Dumps in the Upper Silesian Coal Basin *Land* **10**(1) 23 DOI <https://doi.org/10.3390/land10010023>
- [7] Kostenko V, Zavialova O, Chepak O and Pokalyuk V 2018 Mitigating the adverse environmental impact resulting from closing down of mining enterprises *Mining of Mineral Deposits* **12**(3) 105–112 DOI <https://doi.org/10.15407/mining12.03.105>
- [8] Gopinathan P, Subramani T, Barbosa S and Yuvaraj D 2023 Environmental impact and health risk assessment due to coal mining and utilization *Environmental Geochemistry and Health* **45** 6915–6922 DOI <https://doi.org/10.1007/s10653-023-01744-z>
- [9] Gawor L 2014 Coal mining waste dumps as secondary deposits – examples from the Upper Silesian Coal Basin and the Lublin Coal Basin *Geology, Geophysics & Environment* **40**(3) 285–289 DOI <https://doi.org/10.7494/geol.2014.40.3.285>
- [10] Malashkevych D, Petlovanyi M, Sai K and Zubko S 2022 Research into the coal quality with a new selective mining technology of the waste rock accumulation in the mined-out area *Mining of Mineral Deposits* **16**(4) 103–114 DOI <https://doi.org/10.33271/mining16.04.103>
- [11] Zhu W, Xu J, Xu J, Chen D and Shi J 2017 Pier-column backfill mining technology for controlling surface subsidence *International Journal of Rock Mechanics and Mining Sciences* **96** 58–65 DOI <https://doi.org/10.1016/j.ijrmms.2017.04.014>
- [12] Povzun O, Podkopayev S and Kamenets V 2017 *Naukovo-tekhnichnyy zhurnal* **1**(15) 138–146
- [13] Zubov A, Zubov A and Zubova L 2023 Ecological hazard, typology, morphometry and quantity of waste dumps of coal mines in Ukraine *Ecological Questions* **34**(4) 1–19 DOI <https://doi.org/10.12775/EQ.2023.042>
- [14] Pierzyna P, Popczyk M and Suponik T 2017 Testing the possibility of leaching salt debris obtained from underground excavations *E3S Web of Conferences* **18** 01033 DOI <https://doi.org/10.1051/e3sconf/20171801033>

- [15] Vriens B, Plante B, Seigneur N and Jamieson H 2020 Mine Waste Rock: Insights for Sustainable Hydrogeochemical Management *Minerals* **10**(9) 728 DOI <https://doi.org/10.3390/min10090728>
- [16] Smoliński A, Dombek V, Pertile E, Drobek L, Gogola K, Żechowska S W and Magdziarczyk M 2021 An analysis of self-ignition of mine waste dumps in terms of environmental protection in industrial areas in Poland *Scientific Reports* **11** 8851 DOI <https://doi.org/10.1038/s41598-021-88470-7>
- [17] Karabyn V, Shtain B and Popovych V 2018 *News of the National Academy of Sciences of the Republic of Kazakhstan. Series of Geology and Technical Sciences* **3**(429) 64–74
- [18] Surovka D, Pertile E, Dombek V, Vastyl M and Leher V 2017 Monitoring of Thermal and Gas Activities in Mining Dump Hedvika, Czech Republic *IOP Conference Series: Earth and Environmental Science* **92**(1) 012060 DOI <https://doi.org/10.1088/1755-1315/92/1/012060>
- [19] Róžański Z 2018 Fire hazard in coal waste dumps – selected aspects of the environmental impact *IOP Conference Series: Earth and Environmental Science* **174**(1) 012013 DOI <https://doi.org/10.1088/1755-1315/174/1/012013>
- [20] Rakhimova G, Stolboushkin A, Vyshar O, Stanevich V, Rakhimov M and Kozlov P 2023 Strong Structure Formation of Ceramic Composites Based on Coal Mining Overburden Rocks *Journal of Composites Science* **7**(5) 209 DOI <https://doi.org/10.3390/jcs7050209>
- [21] Daněk T, Jelínek J and Thomas J 2015 Material of Burned Coal Wastes Spoil Heaps As Source of Mullite for Ceramic Industry *MATEC Web of Conferences* **26** 01004 DOI <https://doi.org/10.1051/mateconf/20152601004>
- [22] Hen K, Wang W, Shang Y, Wang H, Ma W and Hao C 2020 Study status and outlook on burnt rock in the ecologically vulnerable coal-mining areas *China mining magazine* **29**(3) 171–176 DOI <https://doi.org/10.12075/j.issn.1004-4051.2020.03.004>
- [23] Chen K, Shao D, Liu Z, Chen L and He G 2023 Experimental study on basic engineering properties of loess improved by burnt rock *Scientific Reports* **13**(1) 11023 DOI <https://doi.org/10.1038/s41598-023-38083-z>
- [24] Malovanyy M, Lyashok Y, Podkopayev S, Povzun O, Kipko O, Kalynychenko V and Skyrda A 2020 Environmental Technologies for Use of Coal Mining and Chemical Industry Wastes *Journal of Ecological Engineering* **21**(2) 95–103 DOI <https://doi.org/10.12911/22998993/116339>
- [25] Panasiuk Y I, Malikov V V and Talakh L A 2019 Physical-mechanical properties of mine production wastes for road construction *Suchasni tekhnolohiyi ta metody rozrakhunkiv u budivnytstvi* **11** 99–106 DOI [https://doi.org/10.36910/6775-2410-6208-2019-1\(11\)-12](https://doi.org/10.36910/6775-2410-6208-2019-1(11)-12)
- [26] Żukowska G, Myszura-Dymek M, Roszkowski S and Bik-Malodzińska M 2023 Effect of Coal Mining Waste and Its Mixtures with Sewage Sludge and Mineral Wool on Selected Properties of Degraded Anthropogenic Soil *Journal of Ecological Engineering* **24**(10) 340–350 DOI <https://doi.org/10.12911/22998993/170949>
- [27] Kostenko V, Bohomaz O and Hlushko I 2022 Preliminary research of the possibility of using solid mine waste as fertilizer *Naukovyy visnyk DonNTU* **1(8)-2(9)** 56–62 DOI [https://doi.org/10.31474/2415-7902-2022-1\(8\)-2\(9\)-56-62](https://doi.org/10.31474/2415-7902-2022-1(8)-2(9)-56-62)
- [28] 1996 State Standard of Ukraine. DSTU BV.2.1-4-96. Soils. Methods of laboratory determination of strength and deformation characteristics
- [29] Kostenko V, Bohomaz O, Hlushko I, Liashok N and Kostenko T 2023 Use of solid mining waste to improve water retention capacity of loamy soils *Mining of Mineral Deposits* **17**(4) 29–34 DOI <https://doi.org/10.33271/mining17.04.029>
- [30] Kostenko V, Lyashok Y, Hlushko I, Bohomaz O, Zavyalova O, Kohtyeva O and Kartavtseva O 2021 Method of organo-mineral fertilizer production Patent for utility model UA 151740